INVESTIGATION OF 10.6 MICRON PROPAGATION PHENOMENA
(2880-4)

The Ohio State University

ElectroScience Laboratory

Department of Electrical Engineering
Columbus, Ohio 43212

Principal Investigator: Dr. Stuart A. Collins
Phone: 614-622-5045

Project Engineer: Raymond P. Urtz, Jr.
Phone: 315-330-3443

AD 731572

DDC
RECEIVED
OCT 22 1971
D

Approved for public release;
distribution unlimited

The views and conclusions in this document are those of the
authors and should not be interpreted as necessarily representing
the official policies, either expressed or implied, of the Advanced
Research Projects Agency or the U. S. Government.

Rome Air Development Center
Air Force Systems Command
Griffiss Air Force Base, New York

38

DOCUMENT CONTROL DATA - R & D

(Security classification of title, body of abstract and indexing annotation must be entered when the overall report is classified)

1 ORIGINATING ACTIVITY *(Corporate author)*	2a. REPORT SECURITY CLASSIFICATION
The Ohio State University ElectroScience Lab. Department of Electrical Engineering Columbus, OH 43212	UNCLASSIFIED
	2b. GROUP

3 REPORT TITLE

INVESTIGATION OF 10.6 MICRON PROPAGATION PHENOMENA
(2880-4)

4 DESCRIPTIVE NOTES *(Type of report and inclusive dates)*

Semiannual Report 8 January 1971 to 8 July 1971

5 AUTHOR(S) *(First name, middle initial, last name)*

6 REPORT DATE	7a. TOTAL NO OF PAGES	7b. NO OF REFS
8 August 1971	30	3

8a CONTRACT OR GRANT NO	9a. ORIGINATOR'S REPORT NUMBER(S)
F30602-70-C-0003	ElectroScience Laboratory No. 2880-4
b. ~~XXXXXXXXX~~ Job Order Number: 12790000	
c. ARPA Order No. 1279	9b OTHER REPORT NO(S) *(Any other numbers that may be assigned this report)* RADC-TR-71-202
d.	

10 DISTRIBUTION STATEMENT

Approved for public release; distribution unlimited.

11 SUPPLEMENTARY NOTES Monitored by: Raymond J. Urtz, Jr. RADC (OCSE), GAFB NY 13440	12 SPONSORING MILITARY ACTIVITY Advanced Research Projects Agency Arlington, VA 22209

13 ABSTRACT

This report summarizes technical details of work performed at the Ohio State University ElectroScience Laboratory during the period January 8, 1971 to July 8, 1971.

Progress is reported on the design, construction, and testing of apparatus and computer software for an experiment on atmospheric imaging and image reconstruction at 10.6 microns. The initial experiment involves recording, in digital format, the atmospherically degraded images of a pair of point sources and is to be applied later to images received from laser illuminated real objects. Both experimental equipment data processing for image reconstruction are discussed. Preliminary data obtained by imaging an atmospherically degraded laser beam during recent tests at the RADC Verona PATS test site are presented.

An analysis of errors resulting from tape drop-out during digital recording using a serial (Miller Code) technique is presented for both linear and logarithmic processing of the analog image data prior to recording. It is shown that linear processing is generally superior for the present digital system and hence is recommended.

14 KEY WORDS	LINK A		LINK B		LINK C	
	ROLE	WT	ROLE	WT	ROLE	WT
10.6 MICRONS Atmospheric Imaging Image Restoration Propagation Turbulence Image Scanning						

INVESTIGATION OF 10.6 MICRON PROPAGATION PHENOMENA
(2880-4)

The Ohio State University
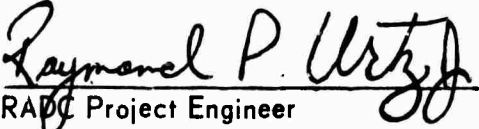ElectroScience Laboratory

ABSTRACT

This report summarizes technical details of work performed at
The Ohio State University ElectroScience Laboratory during the period
January 8, 1971 to July 8, 1971.

Progress is reported on the design, construction, and testing of
apparatus and computer software for an experiment on atmospheric
imaging and image reconstruction at 10.6 microns. The initial experi-
ment involves recording, in digital format, the atmospherically de-
graded images of a pair of point sources and is to be applied later
to images received from laser illuminated real objects. Both experi-
mental equipment and data processing for image reconstruction are
discussed. Preliminary data obtained by imaging an atmospherically
degraded laser beam during recent tests at the RADC Verona PATS test
site are presented.

An analysis of errors resulting from tape drop-out during digital
recording using a serial (Miller Code) technique is presented for both
linear and logarithmic processing of the analog image data prior to
recording. It is shown that linear processing is generally superior
for the present digital system and hence is recommended.

PUBLICATION REVIEW

This technical report has been reviewed and is approved.

Raymond P. Urtz, Jr.
RADC Project Engineer

ii

CONTENTS

I. INTRODUCTION

This is the fourth semiannual technical report on Contract Number F 30602-70-C-0003 entitled "Investigation of 10.6 Micron Propagation Phenomena". This report covers the period January 8, 1971 to July 8, 1971.

The initial aim of this program was to provide theoretical backup information to the RADC Atmospheric Optical Propagation Studies Program. More recently this project has centered on the study of atmospheric imaging and restoration of atmospherically degraded images. The general aim is to provide initial attempts at restoration, to determine potential problems; and to obtain initial data useful for preliminary systems design. Towards this end a system is near completion which will record 10.6 micron images and similarly the software to restore and examine these images.

Primary effort during the past six months has been devoted to the design, construction, and testing of the 10.6 micron imaging system and in writing computer software for processing the experimental data. Detailed descriptions of the basic experiment[1] and of the experimental apparatus[2] have been given in previous technical reports. Tests of the analog portions of the experimental apparatus recently performed at the RADC Verona PATS test site are described and preliminary results of computer analysis of the data thus obtained are presented in the following sections. Changes to the imaging system following the Verona tests are also described and an analysis of the relative merits of linear vs logarithmic pre-processing of the data prior to digital recording is included as an Appendix.

II. IMAGING AND IMAGE RESTORATION APPARATUS

A. Description

The basic experiment to be performed following completion of the experimental apparatus involves simultaneous recording of two atmospherically degraded laser beams.[1] The image received from one beam will be processed to obtain the atmospheric MTF which will then be applied to restore the degraded image received from the second beam. Information on isoplanatic patch size will be obtained by varying the spacing between the two beams and noting the effects on image restoration and by studying the correlation between the two images as a function of beam separation. Later experiments will involve image restoration of reflected images from real objects using a point source reference (laser beam or corner reflector) to obtain the atmospheric MTF, and finally, the use of edge effects in an image to eliminate the need for a reference beam is to be investigated.

1

The experimental equipment described fully in a previous report[2] consists of a two-channel scanning-disc imaging detector capable of simultaneous reception of two separate images using a 40 x 40 element array at 200 frames per second together with real time digitizing, recording, playback, and viewing equipment. Single-channel analog portions of this equipment have recently been completed and successfully tested at the RADC Verona PATS test site as described in the following section. The equipment has now been returned to the OSU ElectroScience Laboratory where the digitizing and recording equipment, the second IR detector, and remaining controls are being incorporated.

One possible change in equipment with respect to that described previously[2] is that the proposed logarithmic video amplifier may be omitted from the final design. This device was included in the original design when analog recording was being considered in order to improve the signal-to-noise ratio of low-level signals. Since digital (Miller Code) recording has been implemented, use of a linear video amplifier is found to be generally superior (see Appendix) as well as simpler and more reliable and hence is recommended.

A second change already incorporated into the equipment is a second set of display electronics, which, together with a second display scope to be supplied by RADC, will permit simultaneous viewing of both video channels simultaneously as well as facilitate system alignment and trouble-shooting.

B. Preliminary System Tests

Single channel analog video tests of the scanning detector were recently conducted at the RADC Verona PATS test site to verify major system design and performance criterion and to obtain preliminary data for checking computer software. The equipment arrangement used for these tests is shown in Fig. 1.

A 10.6 micron laser beam after propagating through the turbulent atmosphere is received by the 16 in. Boller-Chivens telescope and refocussed onto the scanning disc via the positioning and magnifying optics which provide magnifications of 1, 2, or 4 as desired. Energy passing through the scanning disc is converted to an electrical signal by the Cd Hg Te detector, amplified by a preamplifier, further amplified and combined with blanking signals via a video amplifier and is then applied to intensity modulate the display and recording oscilloscopes. Sync signals are also generated by the scanning disc and sync generators and are applied to the raster generator which produces horizontal and vertical digital (point-by-point staircase) deflection voltages for the video display and recording scopes and a blanking signal to turn off the trace between image elements and between frames. The video display scope provides a visual intensity modulated x-y view of the infrared image received by the scanning detector, while the video

2

recording scope provides a line-by-line display which is photographed by a continuous motion strip camera for subsequent analysis using the OSU 16 mm. film digitizer as described later in Section III-D of this report.
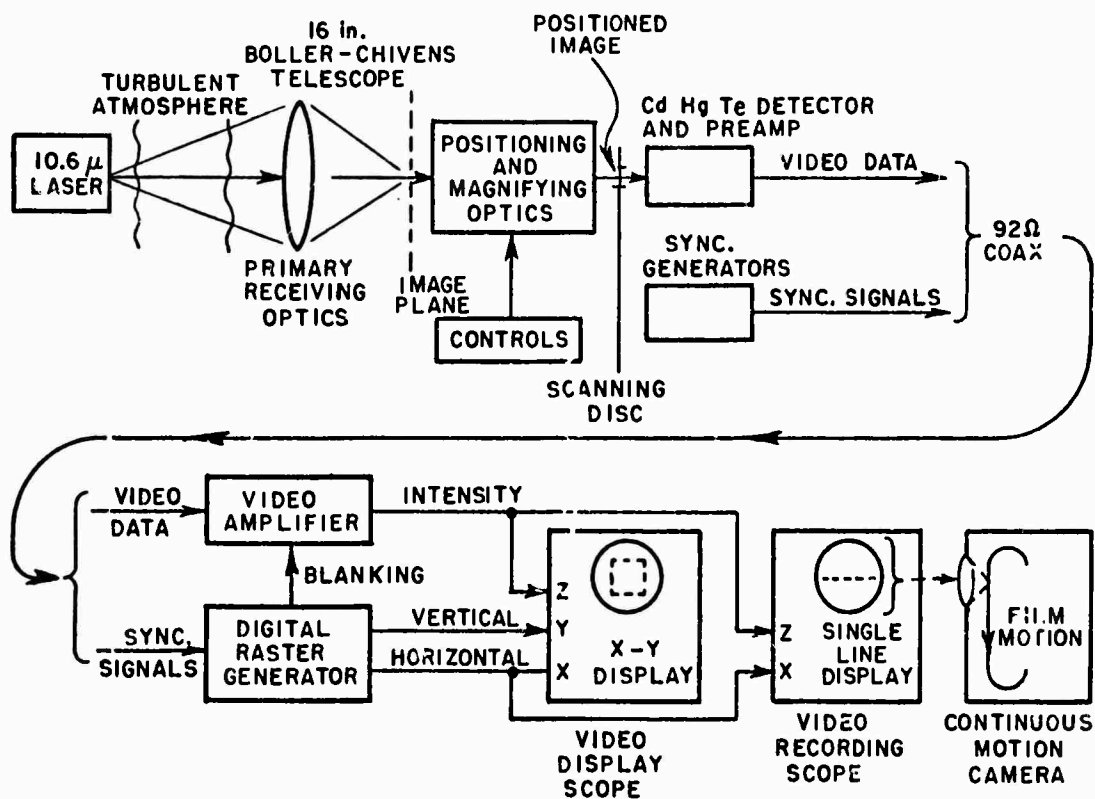
Fig. 1. Experimental arrangement for preliminary tests of the scanning detector.

III. DATA PROCESSING

The overall goal of this program is to study the atmospheric imaging and image restoration processes at 10.6 microns. The imaging equipment described in Section II-A has therefore been developed to record such images. In Sections III-C and D the accomplishments made in restoring these degraded images are described. First though, in Sections III-A and B, basic principles are reviewed from which the equations used by the computer software to restore a degraded image are derived. In Section III-C the computer software developed at the ElectroScience Laboratory is described and in Section III-D some

3

preliminary test results obtained using this software are presented.

A. Image Restoration

This discussion of image restoration is limited to an optical system for which the objects being imaged are incoherently illuminated and the point spread function (PSF) associated with each point contained in a finite region of the object plane is assumed invariant. That is, the object being imaged is assumed to lie entirely within one isoplanatic patch. For present purposes a single 10.6μ laser generated point source is considered. Thus, this point source may be assumed to be either a coherent or an incoherent object   Under these restrictions, each point of the image is a weighted linear superposition of the power distribution associated with that point and all neighboring points in the image plane. For the case considered here, this reduces to the power distribution resulting from a single point in the object plane. The image irradiance (watts/m^2) map obtained by such a system is described by the convolution integral

$$(1) \qquad I_I(x,y) = \int\limits_{-\infty}^{\infty}\!\!\!\int I(x',y') \; P(x-x',y-y') \; dx' \; dy'$$

where $I(x',y')$ is the irradiance map of the ideal image, $P(x-x',y-y')$ is the PSF of the optical system and $I_I(x,y)$ is the resulting irradiance map in the image plane. For an imaging system where the area between the object and image planes is void of atmospheric turbulence effects, the integral in Eq. (1) represents the convolutions of the telescope pupil function with the ideal image irradiance map. However, when atmospheric turbulence is present the system PSF becomes a convolution of the pupil function with the atmospheric PSF which is the case of present interest.

Let $P_S(x-x',y-y')$ be the overall system PSF with atmospheric turbulence effects present, then the image irradiance map in terms of the convolution integral is now

$$(2) \qquad I_I(x,y) = \int\limits_{-\infty}^{\infty}\!\!\!\int I(x',y') \; P_S(x-x',y-y') \; dx' \; dy'.$$

The function of interest here is the ideal image irradiance map, $I(x',y')$. A solution for $I(x',y')$ is easier to obtain if the Fourier Transform of Eq. (2) is used. Such a transform leads to the spatial frequency domain equation

$$(3) \qquad \tilde{I}_I(K_x,K_y) = \tilde{I}(K_x,K_y) \; \tilde{P}_S(K_x,K_y)$$

where the $\sim$ indicates a Fourier Transformed function and K_x and K_y are spatial frequency variables. Here

4

$$(4) \qquad \tilde{P}_S(K_x, K_y) = \tilde{P}(K_x, K_y)\, \hat{\tilde{A}}(K_x, K_y)$$

where $\hat{\tilde{A}}(K_x, K_y)$ is the frequency domain representation of the atmospheric PSF. The spatial frequency domain representation of a PSF is called the Optical Transfer Function (OTF). The Modulation Transfer Function (MTF) is the magnitude of the OTF normalized by the DC spatial frequency component. The MTF may be interpreted as giving an indication of the smallest detail on the object that may be resolved by the optical system.

Equation (3) suggests that the ideal image may be obtained by dividing the transform of the image irradiance map by the system OTF and then performing an inverse Fourier Transform

$$(5) \qquad I(x,y) = F^{-1}\,\{\hat{\tilde{I}}(K_x, K_y)\} = F^{-1}\left\{\frac{\hat{\tilde{I}}_I(K_x, K_y)}{\tilde{P}_S(K_x, K_y)}\right\} .$$

However, any physically realizable system that might be used to record $I_I(x,y)$ and $P_S(x,y)$ will inherently introduce noise into these signals. With the presence of this noise, it is not possible to obtain the exact solution as indicated by Eq. (4). There will be components of $\tilde{P}_S(K_x, K_y)$ which are zero or at least very small while the amplitude of these components contained in the recorded image spectrum will be higher because of noise components present at these points. Calculating components of the restored spectrum using Eq. (4) at such points will greatly amplify the noise components resulting in an unintelligible restored image.

Since an ideally restored image can not be obtained in the presence of noise, an approximately restored image is obtained by replacing the reciprocal of the OTF, found from the recorded data, by a processing function. In the spatial frequency domain, this processing function is equal to the reciprocal of the OTF spectrum for components which are much greater than the noise level, but is such that it greatly attenuates the large amplitude noise components discussed above.

Replacing $1/\tilde{P}_S(K_x, K_y)$ in Eq. (4) by the processing function $\tilde{P}_p(K_x, K_y)$, and realizing that the resultant function will be an approximately restored image, $\tilde{I}_A(K_x, K_y)$ we have

$$(6) \qquad \hat{\tilde{I}}_A(K_x, K_y) = \tilde{I}_I(K_x, K_y)\, \hat{\tilde{P}}_p(K_x, K_y).$$

Further if we assume the form of $\tilde{P}_p(K_x, K_y)$ to be

$$(7) \qquad \tilde{P}_p(K_x, K_y) = \frac{1}{\tilde{P}_S(K_x, K_y)} \; \tilde{P}_0(K_x, K_y)$$

5

then by using this processing function the relationship between the degraded image, the ideal restored image, and the approximately restored image is given by

$$(8) \qquad \tilde{I}_A(K_x, K_y) = \tilde{I}(K_x, K_y)\, \tilde{P}_o(K_x, K_y) = \frac{\tilde{I}_I(K_x, K_y)\, \tilde{P}_o(K_x, K_y)}{\tilde{P}_S(K_x, K_y)}$$

$$= \tilde{I}_I(K_x, K_y)\, \tilde{P}_p(K_x, K_y).$$

We can see from Eq. (8) that the approximate solution now has resolution less than that of the ideal image.

Taking the inverse Fourier Transform of Eq. (8) we find the equation to be solved for the approximate restored image is

$$(9) \qquad I_A(x, y) = F^{-1}\, \{\tilde{I}_I(K_x, K_y)\, \tilde{P}_p(K_x, K_y)\} \quad .$$

The software developed at the ElectroScience Laboratory to restore turbulence degraded images computes each component of the approximate restored image spectrum using

$$(10) \qquad \tilde{I}(K_x, K_y) = \tilde{I}_I(K_x, K_y)/\tilde{P}_S(K_x, K_y)$$

(the inverse of Eq. (5)) and then checks these values against a test value. This test value is determined by looking at the entire spectrum found from Eq. (10) and choosing a level below which all but a few obviously incorrect components are found. All components computed, using Eq. (10), which are less than this test value are included, unaltered, in the spectrum $\tilde{I}_A(K_x, K_y)$; however, if a component exceeds the test value it is considered to be the result of noise amplification as discussed previously and is replaced by a more realistic value found by interpolation of the nearby acceptable values of $\tilde{I}_A(K_x, K_y)$. Thus the $\tilde{P}_o(K_x, K_y)$ factor of the processing function (Eq. (7)) is equal to 1.0 when the spectrum components are less than the preselected test value and equal to some complex constant α, where $|\alpha| \ll 1.0$, for those components that exceed the test value. That is

$$(11) \qquad \tilde{P}_o(K_x, K_y) = \begin{cases} 1.0 \text{ for } \dfrac{\tilde{I}_I(K_x, K_y)}{\tilde{P}_S(K_x, K_y)} < \text{ Test value} \\[20pt] \alpha(|\alpha| \ll 1) \text{ for } \dfrac{\tilde{I}_I(K_x, K_y)}{\tilde{P}_S(K_x, K_y)} > \text{ Test value.} \end{cases}$$

6

Substituting Eq. (11) into Eq. (7) we find the processing function to be

$$(12) \quad \tilde{P}_p(K_x, K_y) = \begin{cases} \dfrac{1}{\tilde{P}_S(K_x, K_y)} & \text{for spectrum components} < \text{test value} \\[2em] \dfrac{\alpha}{\tilde{P}_S(K_x, K_y)} & \text{for spectrum components} \geq \text{test value.} \end{cases}$$

This function does indeed behave according to the format previously stated as desirable for the processing function.

We are thus interested in solving Eq. (9) where $\tilde{P}_p(K_x, K_y)$ is given by Eq. (12)

B. The Fast Fourier Transform

The method of solution proposed in Eq. (9) of the preceding section indicates that a capability for performing a bidirectional Fourier Transform is required. Since the ElectroScience Laboratory imaging hardware generates 1600 discrete samples per image (40 lines/image and 40 samples/line) the transform that must be applied is the (finite) Discrete Fourier Transform (DFT). The defining equation for a two dimensional DFT is

$$(13) \quad \tilde{I}_{IJ} = \frac{1}{N_x N_y} \sum_{R=0}^{N_x-1} \sum_{S=0}^{N_y-1} I_{RS} \, e^{-j2\pi \left(\frac{IR}{N_x} + \frac{JS}{N_y} \right)}$$

where I_{RS} $(R = 0, \cdots N_x-1 \quad S = 0, \cdots N_y-1)$ is a sequence of $N_x N_y$ finite valued complex numbers (discrete samples) and $\tilde{I}_{IJ}$ is the DFT of I_{RS}. The inverse DFT of $\tilde{I}_{IJ}$ is

$$(14) \quad I_{RS} = \sum_{I=0}^{N_x-1} \sum_{J=0}^{N_y-1} \tilde{I}_{IJ} \, e^{j2\pi \left(\frac{IR}{N_x} + \frac{JS}{N_y} \right)}.$$

For the ElectroScience Laboratory system $N_x = N_y = N = 40$ samples.

The validity of this transform pair can be proven by substituting I_{IJ} from Eq. (13) into Eq. (14) and using the orthogonality relationship for exponentials

7

$$(15) \qquad \sum_{I=0}^{N_x-1} \sum_{J=0}^{N_y-1} e^{-j2\pi\left(\frac{IR}{N_x}+\frac{JS}{N_y}\right)} e^{j2\pi\left(\frac{IM}{N_x}+\frac{JN}{N_y}\right)} = $$

$$\begin{cases} N_x N_y & \text{for } R=M \\ & \qquad S=N \\ 0 & \text{otherwise.} \end{cases}$$

Such a DFT pair will be denoted as

$$(16) \qquad I_{RS} \longleftrightarrow \tilde{I}_{IJ} .$$

Two other properties of the DFT pair worth mentioning here are first that I_{RS} and $\tilde{I}_{IJ}$ are periodic with periods of $\pm kN_x$ and $\pm \ell N_y$ ($k,\ell=0,1,...$), and second, that the transforms of two real valued sequences are obtained simultaneously by forming a sample by sample complex sum of the two real sequences and then applying the DFT to this complex sequence.

Although the DFT is a very powerful bidirectional mapping operator, it is very time consuming and hence it is costly to use these transforms directly when a large number of samples are involved as in the case here. To directly apply the DFT to the 1600 data samples from a single two dimensional image would require $N^4 = 2.56 \times 10^6$ complex multiplication and addition operations. Thus, performing the DFT transform necessary to find a restored image becomes a natural application for the Fast Fourier Transform (FFT). The FFT is a highly efficient method of iteratively calculating the coefficients of the DFT by combining progressively larger weighted sums of the sampled data. The approximate number of complex multiplications and additions necessary for calculating a two dimensional FFT is $4N_0^2 \log_2 N_0$ [3]. However, for the FFT, the number of samples, N_0, must be an integral power of two. Thus to include all 40 x 40 samples generated by the ElectroScience Laboratory equipment, these 40 x 40 samples must be placed in the center of a 64 x 64 sample input to the FFT with samples not in the 40 x 40 array being set equal to zero. The number of operations necessary to calculate the FFT for $N_0 = 64$ is approximately 9.8×10^4, or less than 4% of the operations necessary to calculate the DFT directly. Cochran[3] et al also point out that not only are the number of calculations and hence the computational time reduced by this factor, but also round off errors are reduced by the same factor.

The particular FFT algorithm used here is one supplied in IBM's FORTLIB library; the subroutine is called FOUR2 and is based on the Cooley-Tukey FFT. FOUR2 computes the DFT of a single precision input data array where, for the present case of interest, this array represents samples taken from one cycle of the periodically extended two-

8

dimensional image. By merely changing one parameter in the calling statement for FOUR2 either the DFT or inverse DFT is computed.

C. Computer Software

Computer software for restoring turbulence degraded images has been developed at the ElectroScience Laboratory. This software is written in Fortran IV G level for the Ohio State University IBM 360/75 computer. The program is not yet finalized since there will undoubtedly be some changes required once actual digital data from the ESL Miller Code system is available for analysis. However, the general format described here for the computer processing steps should not require changes.

The basic program format is given in Fig. 2. A pair of sampled images are first read in where the PSF is denoted as Image 1 and the degraded image as Image 2. These 40 x 40 discrete sample arrays are each centered in a 64 x 64 array (the FFT subroutine requires that each array dimension equal an integral power of two) and the remaining elements are set equal to zero. The center of gravity of each image is then calculated from which two parameters representing the difference in the x and v coordinates of the two centers of gravity are obtained

(17)   TN2 = shift in x-coordinates

(18)   TN1 = shift in y-coordinates.

These parameters are later used to alter the phase of the Image 2 spectrum so that the transformed Image 2 will have its center of gravity at the same location as the PSF (Image 1).

The complex sum of the two real images is formed and the FFT is taken of this sum. The resulting spectrum is then unraveled to obtain the spectrum of Image 1 (i.e., the OTF) and that of Image 2. The spectrum of the restored image is next calculated by using Eq. (10) and testing to see that no component exceeds the test value (see Section III-C.). When a component does exceed this value, it is replaced by a more realistic value derived from the valid neighboring lower-frequency spectrum components. The result is an approximate spectrum for the restored image as described previously.

The resulting spectrum is transformed back to the x-y spatial coordinate system and an IBM subroutine PLOT3D then outputs this data in the proper form to be used as input data to the SDS 910 plotter. The result is a three-dimensional plot of the restored image. For visual comparison purposes, the degraded image and the system PSF are also displayed similarly in three-dimensional plots.
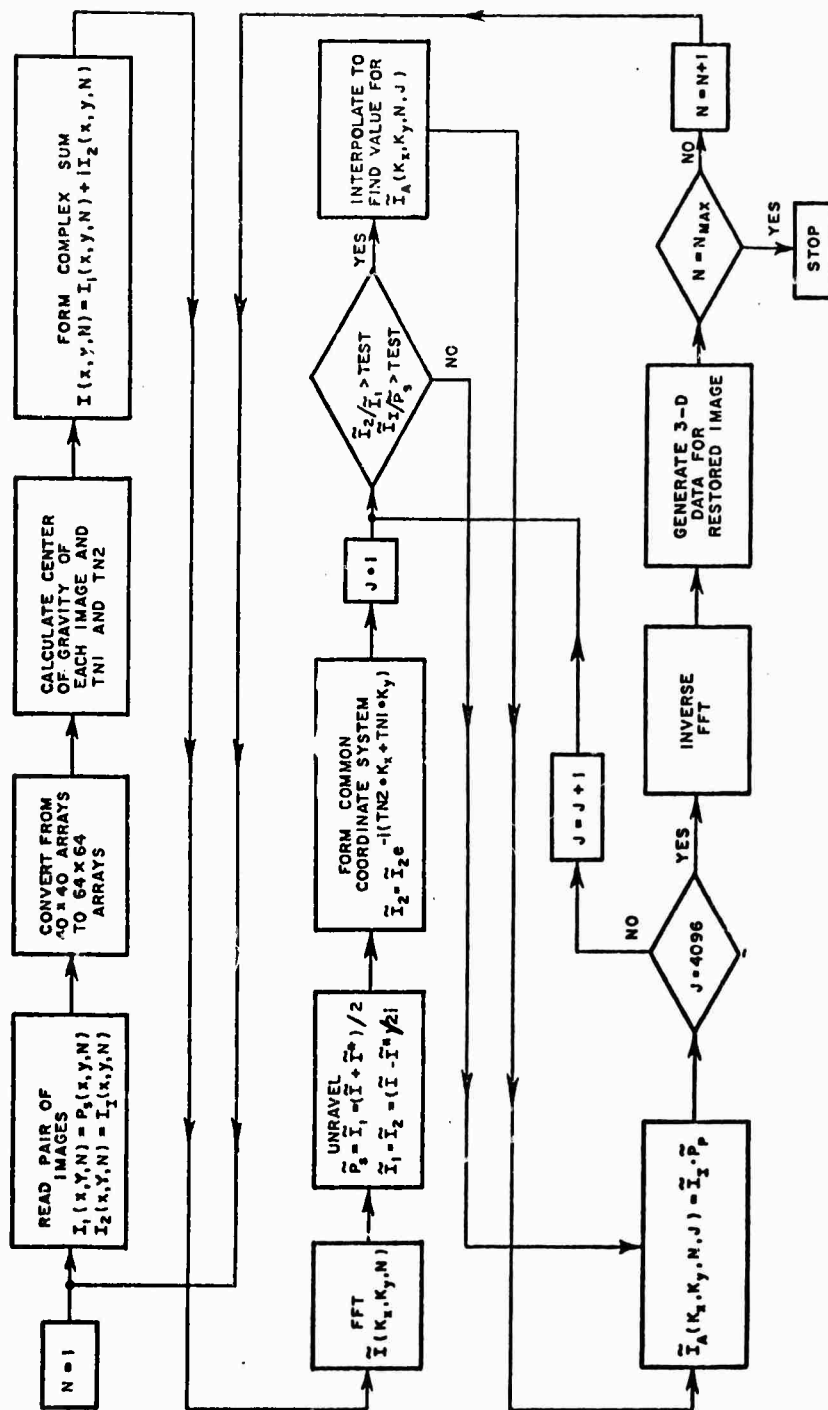
9

Fig. 2. Basic computer program for image restoration.

10

Some of the particular areas of the program that may be altered at a later time are the read-in and display methods and possibly the form of the processing function. It is also possible that information other than the restored image and its spectrum may be desired later. Quantities such as the system MTF and the correlation between restored images as a function of time or horizontal displacement (for the twin beam experiment) are now available from the general program when desired.

In the following section of this report the general program format is adapted to the specific task of processing data scanned and digitized from degraded images recorded on photographic film.

D. Preliminary Test Results

Preliminary tests of the ElectroScience Laboratory 10.6μ scanning detector were performed at the RADC Verona PATS test site during April and May 1971 as described in Section II-B. Using the RADC 1000 foot outdoor propagation range and a 10.6μ laser source, the equipment was set up to display and photograph the turbulence degraded laser spot (see Fig. 1). Only the video intensity and horizontal sweep voltages were applied to the oscilloscope for photographic recording. The vertical sweep was supplied by the constant film motion traveling from top to bottom with respect to the display scope. Although the human eye sees the crt display, with the vertical sweep applied, (Video display scope of Fig. 1) as a 40 x 40 element picture of a turbulence degraded spot, because of the vertical interlace used by the scanning disc and raster generator this image is actually generated by displaying the odd scan lines of the image on a vertical down-scan (i.e., 1, 3, ..., 39) followed by the even scan lines on a vertical up-scan (i.e., 40, 38, ..., 2). Thus when viewing the data recorded by the continuous motion camera we see two consecutive half-images, one essentially the mirror image of the other, which compose a single full image.

Upon receiving the filmed data at the ElectroScience Laboratory, it was reviewed visually to select several sections of interest to be used as test data for the image processing computer software. The selected sections of film were then digitized using the ESL's digital film analyzer which scanned each half-image and recorded the resulting array of 6-bit digital samples on IBM 7-track magnetic tape. This tape then served as the input to a modified version of the image restoration computer software.

Briefly, these software modifications consist of a series of subroutines which read the half-frame data off the magnetic tape, interlace the two half-images to form a single 40 x 40 sample image, and then convert this photographically negative image to a photographically positive image.

11

The first test of the computer software was performed by using the same image as both the degraded image and the system PSF. Such a restoration physically means that the point source of unity magnitude from which the PSF was derived is being restored. We would expect this restored image to be a delta function of unity magnitude and indeed this is the result obtained using the image processing software. Figure 3 is a three-dimensional intensity plot of this restored point source. Also included are the PSF and the degraded image respectively, in Fig. 4 and Fig. 5. Note that these are actually the same function in this instance.

The next test was conducted by choosing a particular image as the PSF and then restoring a degraded image recorded 1/200 sec later in time. An example case is shown below. Figure 6 is the system PSF, Fig. 7 is the degraded image, and Fig. 8 is the resulting restored image obtained using the ESL image processing software.

Figures 9a and 9b show the principle cuts through the restored image in Fig. 8. These principle cuts clearly show the restored image in the presence of noise.

Obviously this test case does not represent the true method of image restoration since in the actual situation the degraded image to be restored and the system PSF would be recorded simultaneously. However, the results above do indeed present verification that the computer software is functioning properly.

IV. SUMMARY

This report has described work performed during the last six months in construction and testing of equipment and in writing computer software for experiments in the 10.6 micron imaging and image restoration. Tests recently completed at RADC of the scanning detector and analog video display are described, and samples of the resultant data for an atmospherically degraded laser beam both before and after restoration using the ElectroScience Laboratory computer software are presented. Work now in progress for completing the experimental system and experiments then to be performed are summarized.
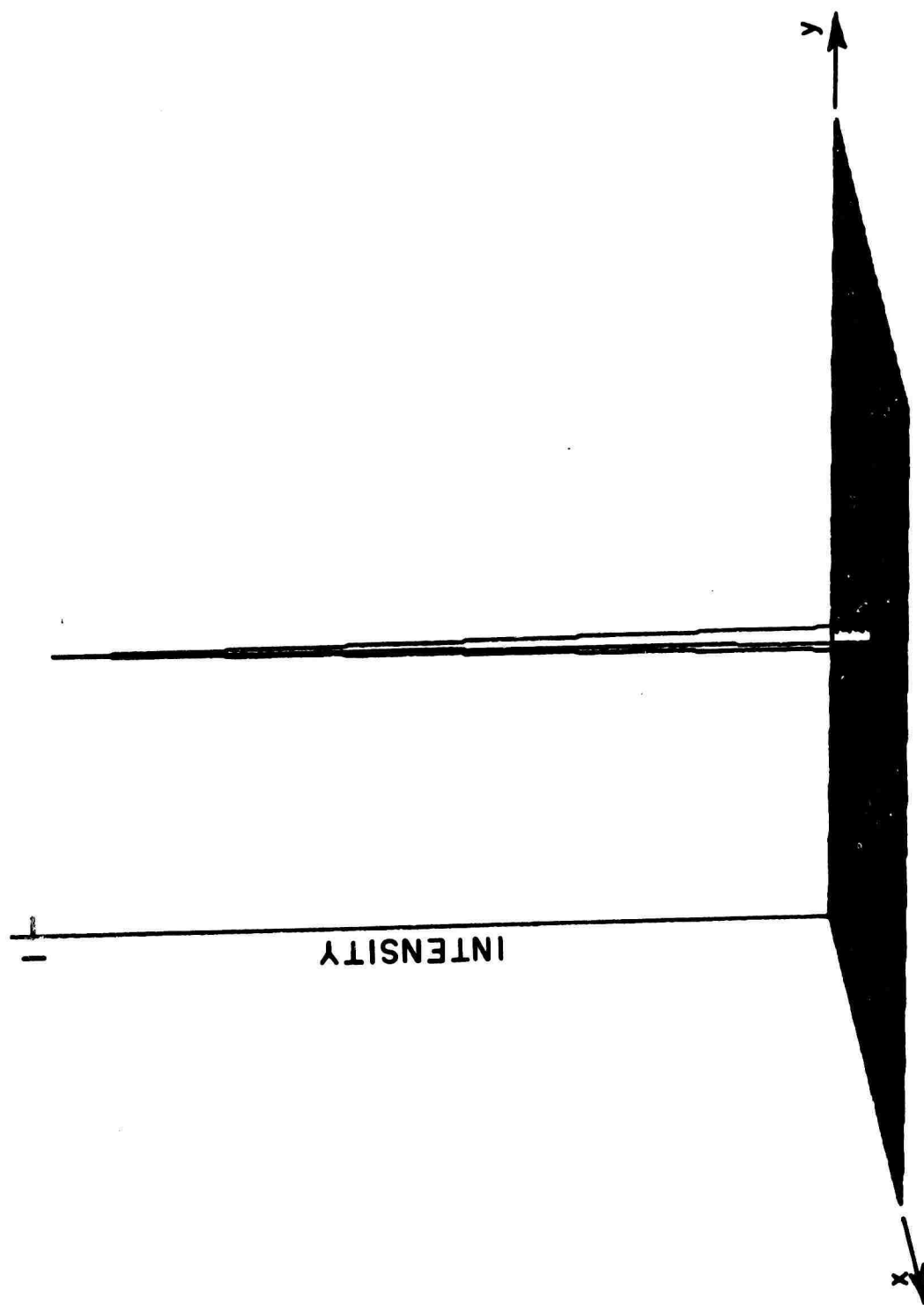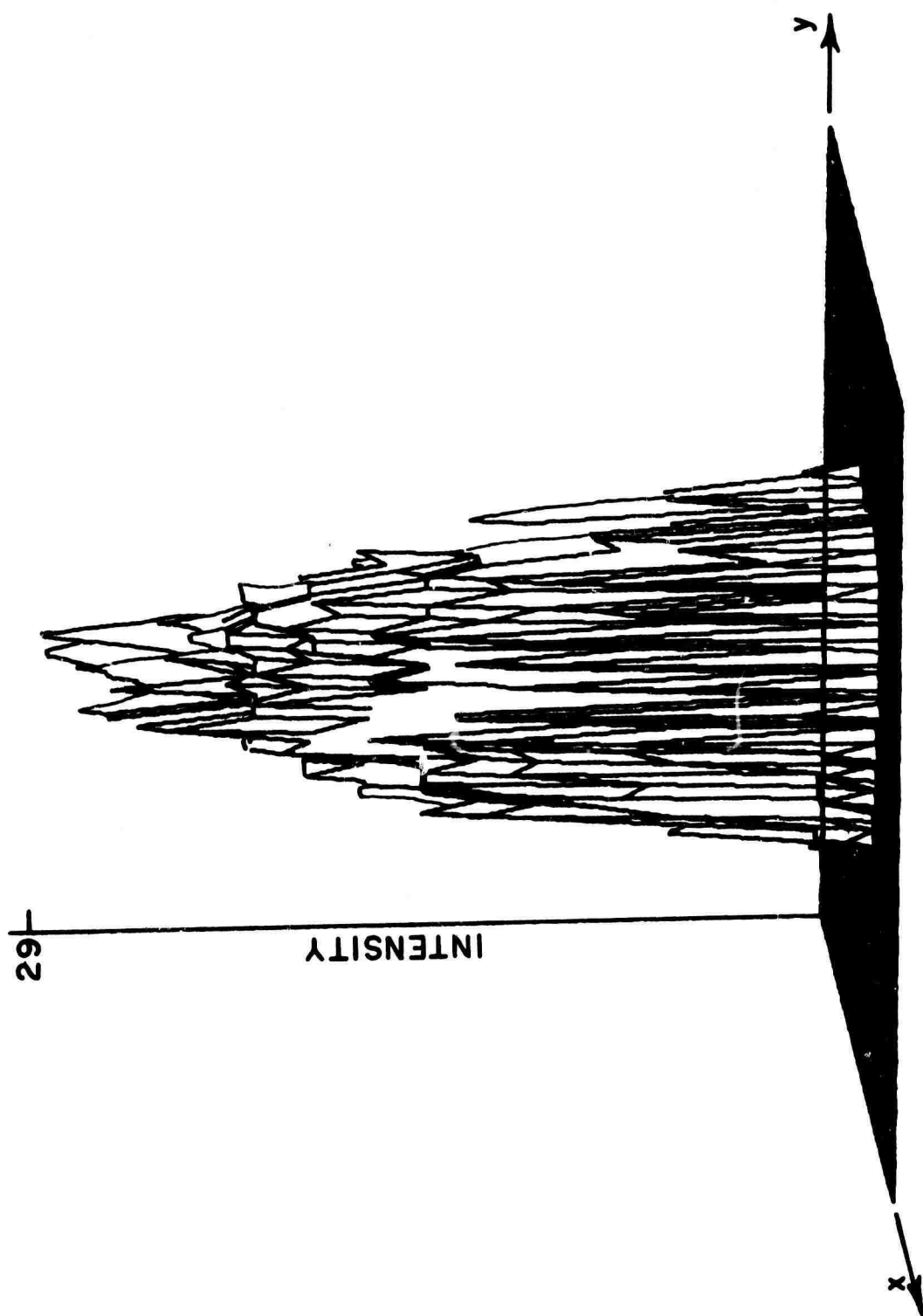
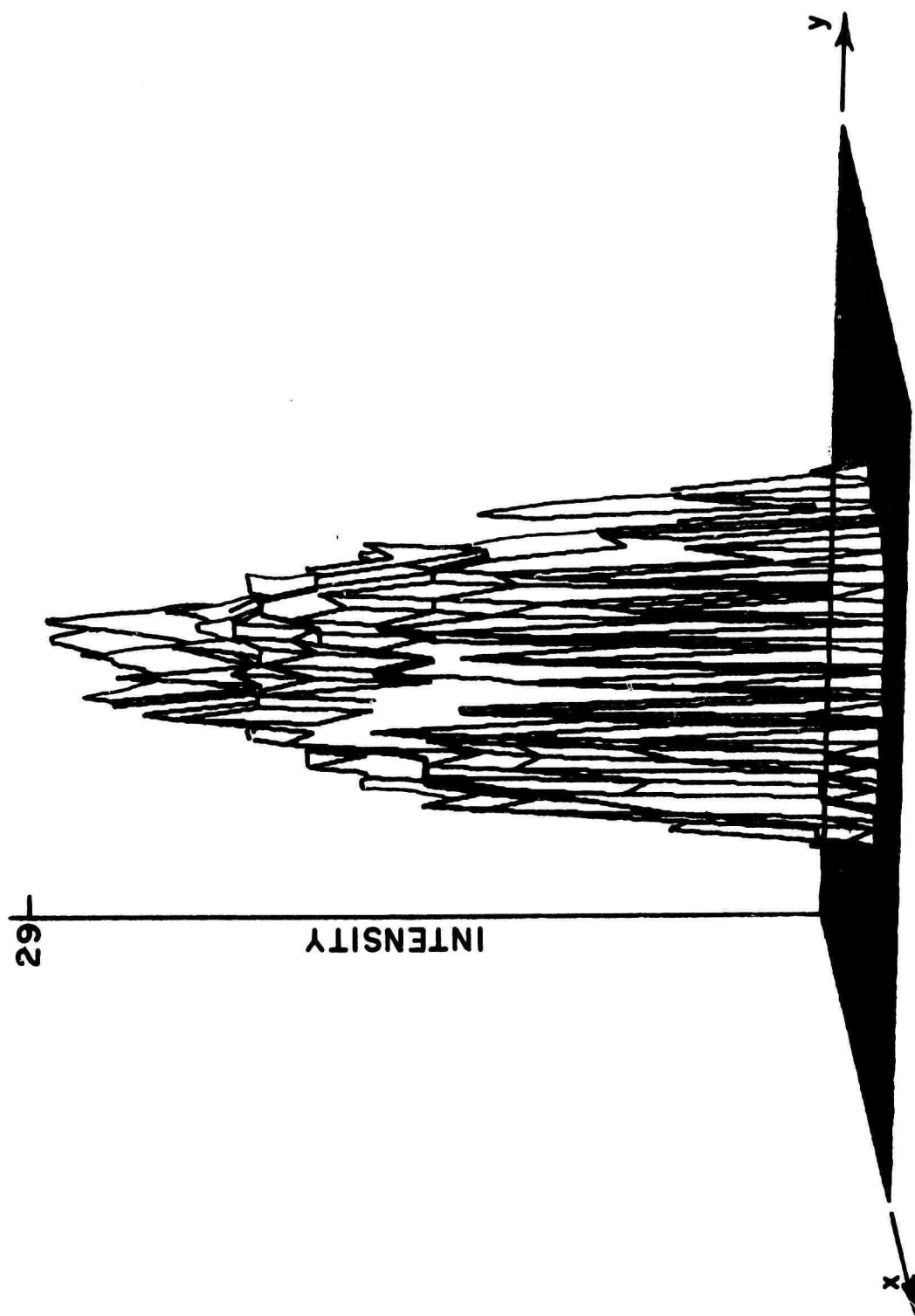Fig. 3. Restored unit intensity point source.

Fig. 4. System PSF.

29

INTENSITY
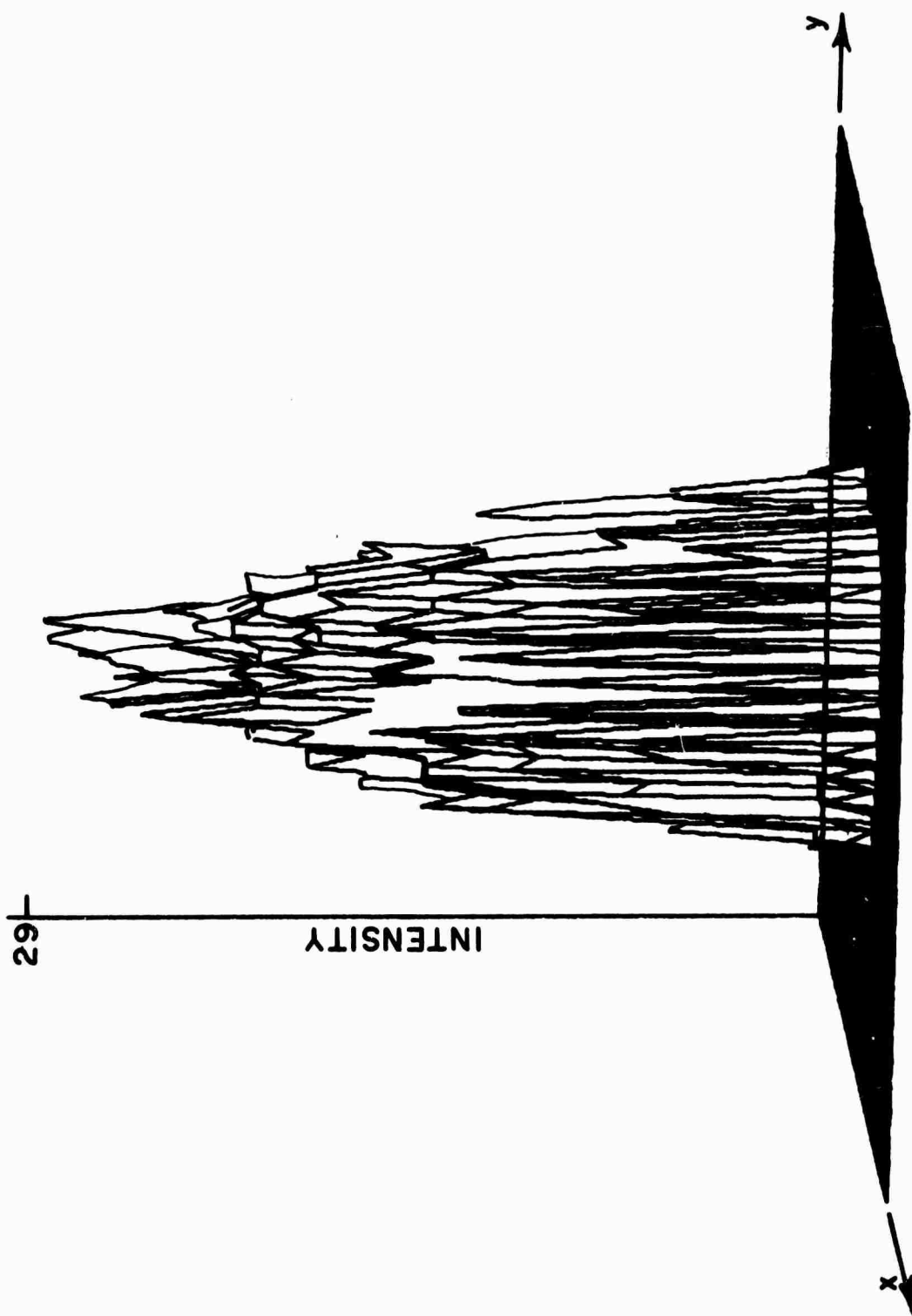
14

Fig. 5. Turbulence degraded image.
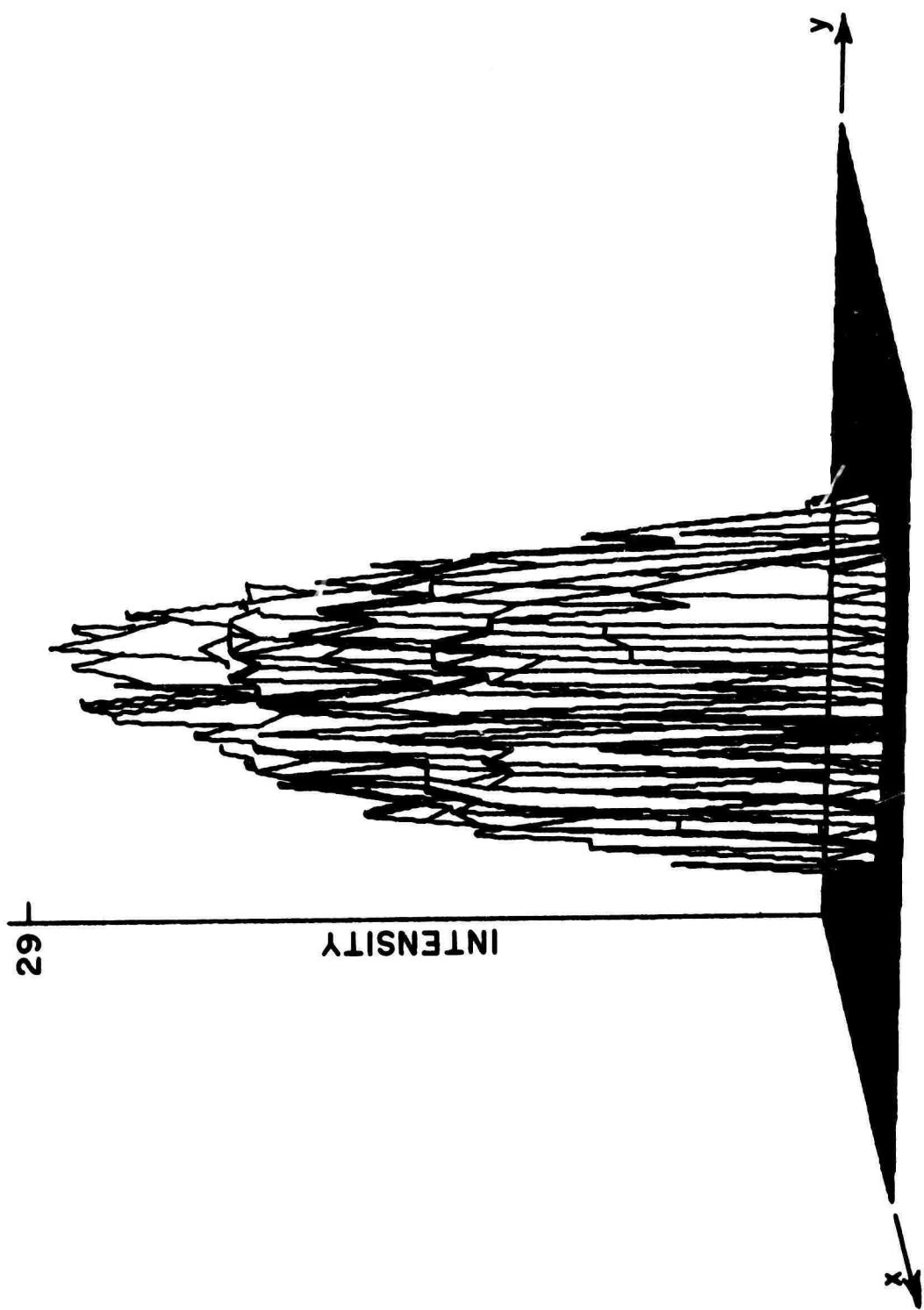
15

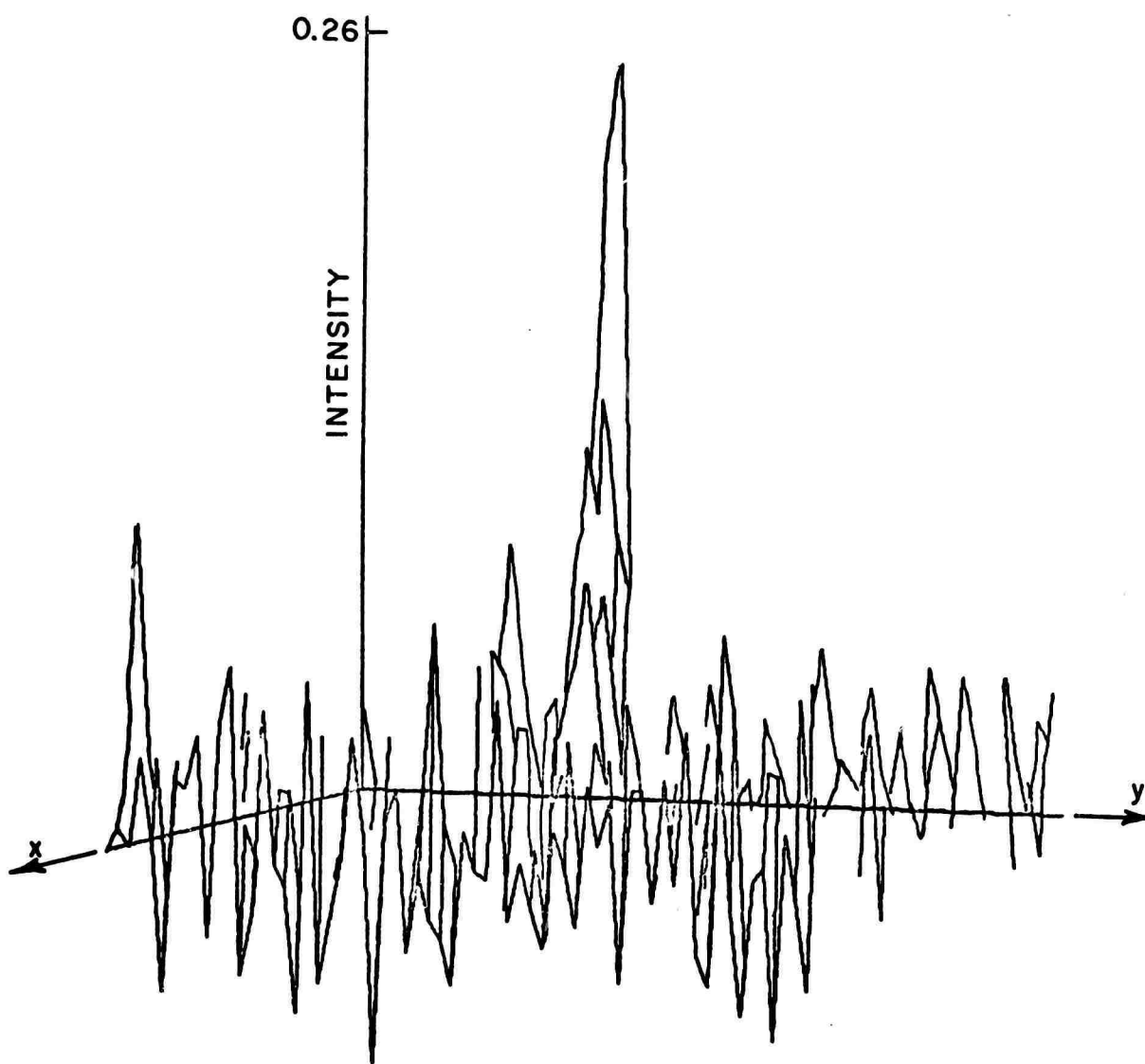Fig. 6. System PSF.

16

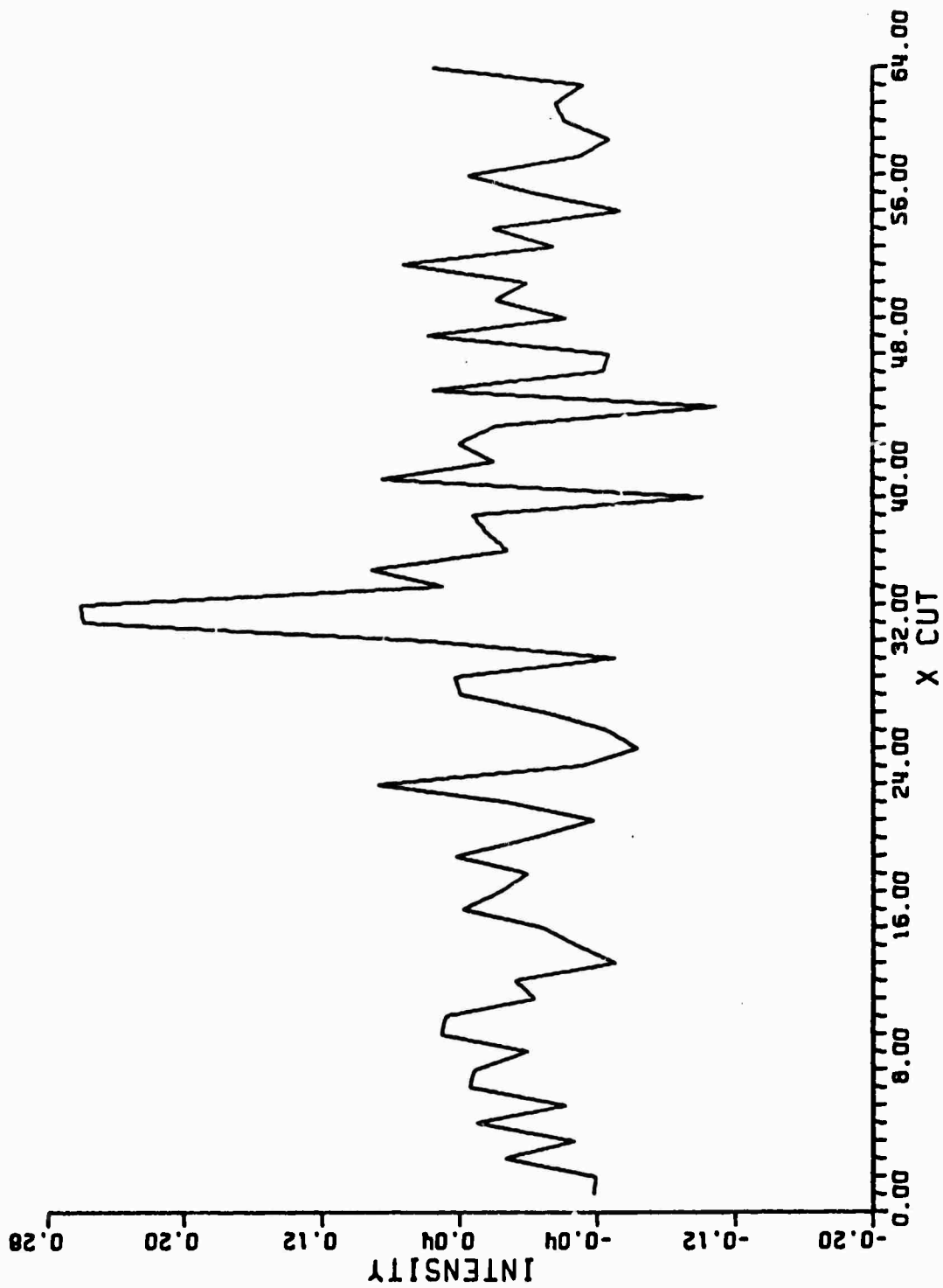Fig. 7. Turbulence degraded image.

17

Fig. 8. Restored image.
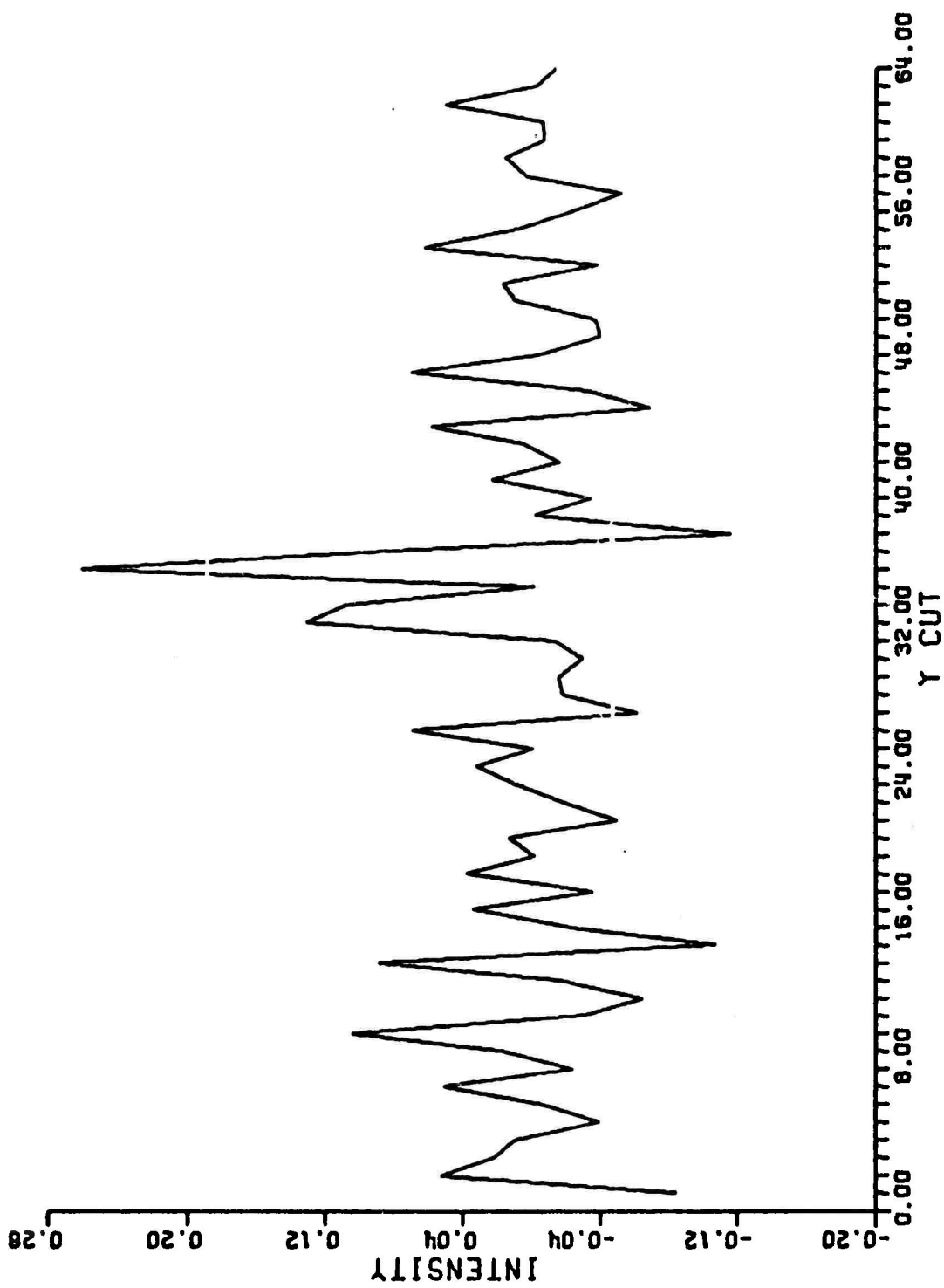
Fig. 9a. Principle x cut thru restored image in Fig. 8.

19

Fig. 9b. Principle y cut thru restored image in Fig. 8.

ERROR ANALYSIS FOR DIGITAL RECORDING USING
LINEAR OR LOGARITHMIC PREPROCESSING OF THE IMAGE DATA

The relative merits of linear or logarithmic amplfication of the
video signals from the preamplifier (see Fig. 1) prior to recording
are considered in this appendix. Two types of system errors are
derived and compared for a digital (Miller Code) recording system
using linear amplification and an equivalent system using logarithmic
amplification. First a system is considered where the only error
results from a bit being dropped during recording or playback. Next,
this same system is considered with respect to the aperture error
associated with analog to digital conversion.

I. DIGITAL SYSTEM DROP-OUT ERRORS

The Computer Laboratory Model HS 802 8 bit Analog to Digital
(A/D) converter used in the ElectroScience Laboratory system has a
maximum unipolar input voltage range of 2048 mv. Thus, the weight
of a least significant bit (LSB) is

$$(19) \qquad 1 \text{ LSB} = \frac{2048 \text{ mv}}{2^8} = 8 \text{ mv}.$$

Let W denote this weighting factor and $V_{A/D}$ denote the maximum input
voltage to the A/D converter.

It has been found from previous tests on the ESL system that
the minimum signal, due to black body radiation from the scanning
disc, at the output of the Perry preamp (see Fig. 1) is approximately
0.35 mv peak and the maximum signal output of this preamp is 1.4 volts
peak. Thus let

$$(20) \qquad v_{max} = 1.4v$$

and

$$(21) \qquad v_{min} = 0.35 \text{ mv}.$$

A. Digital System with Linear Amplification (Fig. 10a)

Let

$$(22) \qquad V_c = k \ v_c$$

be the correct output from the Miller Code decoder and let

LINEAR SCHEME

DETECTOR — PRE AMP —→ v —→ AMP k —→ $V = kv$ —→ A/D — MILLER CODE

(a)

LOG SCHEME

DETECTOR — PRE AMP — LOG AMP — AMP k_0 — A/D — MILLER CODE

v $\alpha \log v + \beta$ $S = k_0 (\alpha \log v + \beta)$

(b)
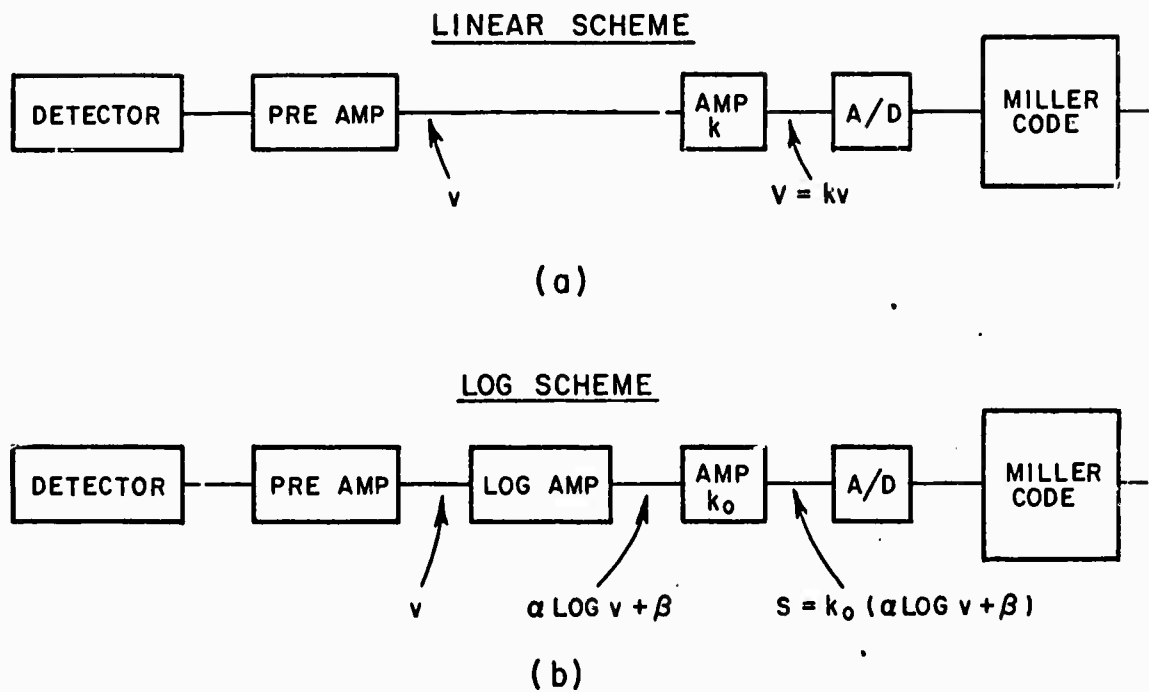
Fig. 10. Block diagram of linear and logarithmic amplification schemes.

(23) $V_e = kv_e$

be an incorrect output from the same decoder when a bit has been dropped from V_c. Amplifier gain k is adjusted so that for an input of $v = v_{max}$ the amplifier output is $V_{A/D}$. Thus

(24) $k = \dfrac{V_{A/D}}{V_{max}}$.

Now consider an 8-bit digital word

	MSB							LSB
Bit Number	8	7	6	5	4	3	2	1
Weight	128	64	32	16	8	4	2	1
Voltage Value	$W2^7$	$W2^6$	$W2^5$	$W2^4$	$W2^3$	$W2^2$	$W2^1$	$W2^0$.

If the signal V_e is a digital output resulting from the loss of the bit with a voltage value of $W2^n$ then the error is

(25) $E_1 = V_c - V_e = V_c - (V_c - W2^n) = W2^n.$

In terms of v_c and v_e this is

(26) $\Delta_1 = v_c - v_e = \dfrac{E_1}{k} = \dfrac{W2^n}{k}$

where $n = 0, 1, 2, \ldots, 7$.

B. <u>Digital System with Logarithmic Amplification (Fig. 10b)</u>

Let

(27) $S_c = k_0 \, (\alpha \log v_c + \beta)$

be the correct output from the Miller Code decoder and let

(28) $S_e = k_0 \, (\alpha \log v_e + \beta)$

23

be an incorrect output from the same Miller Code decoder when a bit has been dropped from S_c. Amplifier gain k_0 is adjusted so that for an input of $v = v_{max}$ the log amplifier output is $V_{A/D}$. Thus

$$(29) \qquad k_0 = \frac{V_{A/D}}{d \log v_{max} + \beta} \quad .$$

If this signal S_e is a digital output resulting from the loss of the bit with a voltage value of $W2^n$ then the error is

$$(30) \qquad E_0 = S_c - S_e = S_c - (S_c - W2^n) = W2^n.$$

In terms of v_c and v_e this is

$$(31) \qquad E_0 = k_0(\alpha \log v_c + \beta) - k_0(\alpha \log v_e + \beta) = W2^n$$

$$(32) \qquad E_0 = k_0\alpha \log v_c/v_e = W2^n$$

or

$$(33) \qquad v_e = v_c \, 10^{-\frac{W2^n}{k_0\alpha}}$$

and hence the error in terms of v_c and v_e is

$$(34) \qquad \Delta_0 = v_c - v_e = v_c \left(1 - 10^{-\frac{W2^n}{k_0\alpha}}\right)$$

where $n = 0, 1, \cdots 7$.

C. Comparison of Drop-out Errors for Linear and Logarithmic Systems

For the digital system with error resulting from the loss of a bit during decoding we have for linear amplification

$$(35) \qquad \Delta_1 = \frac{W2^n}{k}$$

and for logarithmic amplification

$$(36) \qquad \Delta_0 = v_{in} \left(1 - 10^{-\frac{W2^n}{k_0\alpha}}\right) \quad .$$

24

A comparison between Δ_1 and Δ_0 will now be made where the log amplifier chosen is described in Texas Instrument's Bulletin No DL-S 7111427 (page 6). This amplifier has an 80 dB range and the transfer characteristic is plotted here in Fig. 11. From this curve we find

$$(37) \qquad \alpha = \frac{1}{8}$$

$$(38) \qquad \beta = \frac{1}{2} \quad .$$

Next the gains k and k_0 are calculated to be

$$(39) \qquad k = \frac{V_{A/D}}{v_{max}} = \frac{2.048}{1.4} = 1.46$$

and

$$(40) \qquad k_0 = \frac{V_{A/D}}{\log v_{max} + \beta} = \frac{2.048}{.52} = 3.94.$$

Hence we have for the linear system

$$(41) \qquad \Delta_1 = \frac{W2^n}{k} = \frac{8 \times 10^{-3} \, 2^n}{1.46} = 5.47 \times 10^{-3} \, 2^n$$

and for the logarithmic system

$$(42) \qquad \Delta_0 = v_{in}\left(1 - 10^{-\frac{W2^n}{k_0\alpha}}\right) = v_{in}\left(1 - 10^{-16.2 \times 10^{-3} \, 2^n}\right)$$

These curves are plotted in Fig. 12 for $v_{in} = v_{max}$ and for $v_{in} = 0.1 \, v_{max}$. From Fig. 12 it is seen that for the lower bits (i.e., $n = 0, 1, 2, 3, 4$) the error associated with the logarithmic system is greater than that for the linear system until the input signal drops to approximately $0.1 \, v_{max}$ or lower. Note that the apparent improvement for the higher order bits when using the log amplifier for the low input signal levels as indicated by the curves are not applicable when considering bit dropout since, for low signal levels, the high order bits are not used. Hence the improvement obtainable by using the logarithmic amplifier, even at low signal levels, is slight. The linear amplifier is therefore recommended for the present system.
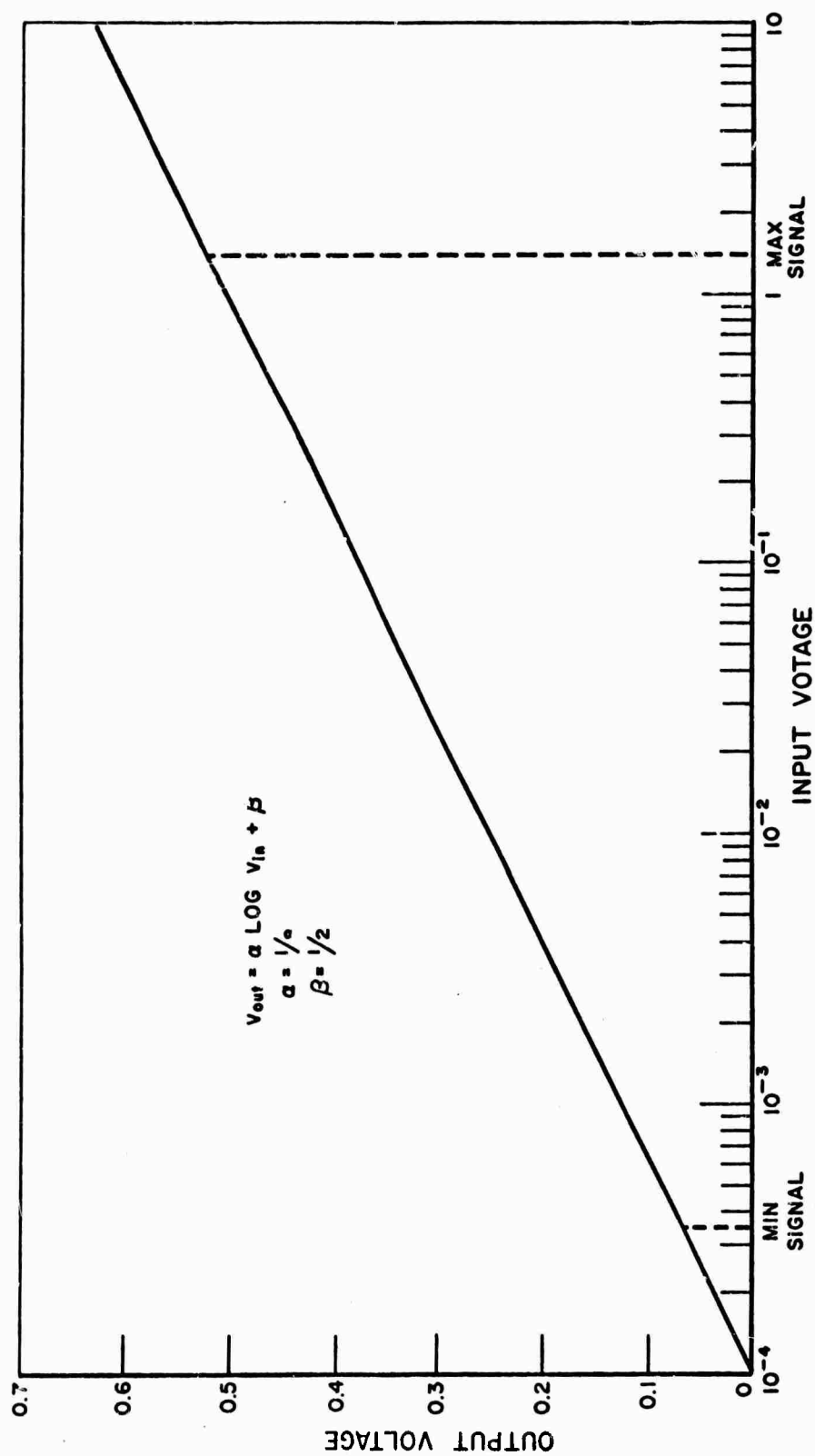
25

Fig. 11. Transfer characteristics for TI 80 dB log amp.
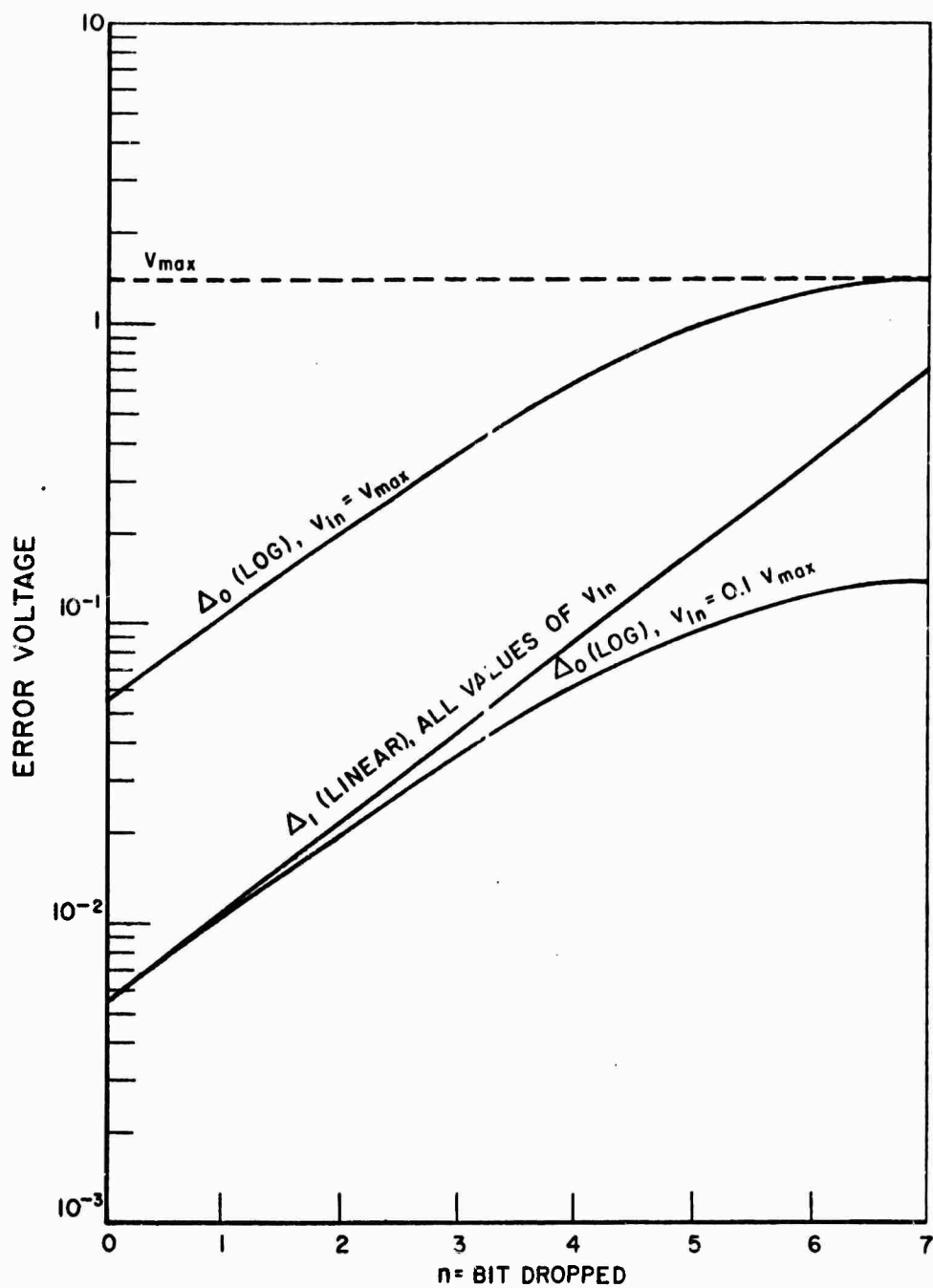
26

Fig. 12. Error voltage vs bit dropped for
linear and log systems.

27

II. APERTURE ERROR

Aperture error for an A/D converter is defined as

$$(43) \qquad E = ta \frac{dv}{dt}$$

where ta is the maximum aperture time and v is the input to the A/D converter.

For the linear amplification scheme (Fig. 10a), the input to the A/D converter is

$$(44) \qquad V = kv$$

and the aperture error is therefore

$$(45) \qquad \psi = ta \frac{dV}{dt} = ta \, k \frac{dv}{dt}$$

assuming constant gain.

Next consider the aperture error associated with the logarithmic amplification scheme (Fig. 10b) where the input to the A/D converter is given by

$$(46) \qquad S = k_0 \, (\alpha \log v + \beta).$$

Aperture error for this case is

$$(47) \qquad \Phi = ta \frac{dS}{dt} = k_0 \, ta \frac{\alpha \log e}{v} \frac{dv}{dt}$$

again assuming constant gain. Now consider the case for which the amplifier input is

$$(48) \qquad v = 1.4 \sin \omega_0 t$$

where

$$(49) \qquad \omega_0 = 2\pi \times 1.6 \times 10^5.$$

This represents the highest amplitude and highest frequency component expected as an input in the ElectroScience Laboratory system.

The Computer Laboratory Model HS 802 8-bit A/D converter has a maximum aperture time

28

(50) $t_a = 10^{-9}$ sec

thus for the linear scheme the aperture error is

(51) $\Psi = 1.4\ t_a\ k\ \omega_0 \cos \omega_0 t$

from which

(52) $\Psi_{max} = 1.4\ t_a\ k\ \omega_0 = 2.04$ mv

while for the logarithmic scheme the aperture error is given by

(53) $\Phi = k_0\ t_0\ \alpha\ \omega_0 \log e\ \dfrac{\cos \omega_0 t}{\sin \omega_0 t}$.

Equation (53) indicates that the maximum value of Φ can be infinite if a sample is taken at the wrong time, i.e., when the input voltage is passing through zero. This, of course does not happen in practice since no realizable amplifier remains logarithmic for zero input voltage. For a practical logarithmic amplifier, aperture error would in general be greater for low level input signals and somewhat smaller for high level signals than when a linear amplifier is used. Since aperture error for the linear system is approximately 1/4 the value of the least significant bit, this error should be negligible for either the linear or logarithmic amplifier in the present system.

REFERENCES

1. "Investigation of 10.6 Micron Propagation Phenomena,"
    (Semiannual Report), Report 2880-1, March 1970, The Ohio
    State University ElectroScience Laboratory, Department of
    Electrical Engineering; prepared under Contract F30602-70-
    C-0003 for Rome Air Development Center. (AD 869 474)

2. "Investigation of 10.6 Micron Propagation Phenomena,"
    (Semiannual Report), Report 2880-3, February 1971, The Ohio
    State University ElectroScience Laboratory, Department of
    Electrical Engineering; prepared under Contract F30602-70-
    C-0003 for Rome Air Development Center.

3. Cochran, William T., et al., "What is the Fast Fourier
    Transform?", IEEE Transactions on Audio and Electroacoustics,
    Vol. AU-15, No. 2, June 1967, pp. 45-56.